minerals

MDPI

Article

The Efficiency of Black Mass Preparation by Discharge and Alkaline Leaching for LIB Recycling

Tiaan Punt *, Steven M. Bradshaw, Petrie van Wyk and Guven Akdogan

Department of Process Engineering, Stellenbosch University, Private Bag X1, Matieland 7602, South Africa; smb@sun.ac.za (S.M.B.); apvanwyk@sun.ac.za (P.v.W.); gakdogan@sun.ac.za (G.A.)
* Correspondence: tpunt@sun.ac.za

Abstract: Lithium-ion batteries (LIBs) are dangerous to recycle, as they pose a fire hazard when cut and contain various chemical hazards. If recycled safely, LIBs provide a rich secondary source for metals such as lithium and cobalt, while reducing the environmental impact of end-of-life LIBs. Discharging the spent LIBs in a 5 wt.% NaCl electrolyte at room temperature enables their safe dismantling. A sludge was observed to form during the LIB discharging, with a composition of 34.9 wt.% Fe, 35 wt.% O, 17.7 wt.% Al, 6.2 wt.% C, and 4.2 wt.% Na. The average electrolytic solution composition after the first discharge cycle contained only 12.6 mg/L Fe, 4.5 mg/L Li, 2.5 mg/L Mn, and trace amounts of Ni and Co. Separating the active cathode powder from the aluminum cathode with a 10 wt.% NaOH leach produced an aqueous filtrate with an Al metal purity of 99.7%. The leach composition consisted of 9558 mg/L Al, 13 mg/L Li, 8.7 mg/L Co, and trace amounts of Mn and Ni. The hydrometallurgical sample preparation processes in this study enables the production of a pure black mass with less than 0.05 wt.% Co, 0.2 wt.% Li, 0.02 wt.% Mn, and 0.02 wt.% Ni losses from the active cathode material.

Keywords: lithium-ion batteries; recycling; hydrometallurgy; black mass; alkaline leach

Citation: Punt, T.; Bradshaw, S.M.; van Wyk, P.; Akdogan, G. The Efficiency of Black Mass Preparation by Discharge and Alkaline Leaching for LIB Recycling. *Minerals* **2022**, *12*, 753. https://doi.org/10.3390/min12060753

Academic Editor: Kenneth N. Han

Received: 6 May 2022
Accepted: 9 June 2022
Published: 14 June 2022

1. Introduction

Since the commercialisation of lithium-ion batteries (LIBs) in the 1990s for portable electronic devices such as cellular phones and laptops, their increasing energy density and decreasing cost has led to a surge in their popularity [1]. Due to the cost effectiveness and favourable properties of LIBs, such as high energy density and low weight to volume ratio [2], their adoption for hybrid and electric vehicles (EVs) has further accelerated the growth of the LIB market. The global lithium-ion battery market is projected to increase from $41.1 billion to $116.6 billion by 2030, with a compound annual growth rate of 12.3% from 2021 to 2030 [3,4]. The large volumes of LIBs will lead to significant waste streams after the LIBs reach their end-of-life, as predictions indicate 11 million tonnes of LIBs will have been discarded worldwide by 2023 [5], with 464,000 tonnes discarded annually by 2025 [6].

LIBs contain components that are classified as hazardous and toxic for human health as well as the environment. LIBs can therefore not be disposed of in general waste to landfill sites, as this may lead to the contamination of underground water with heavy metals, such as cobalt, copper, and nickel, which are the main contributors to the total hazard potential of LIBs [7]. Improper disposal of LIBs can also lead to the production of gases such as HF, Cl_2, CO_2, and CO from the electrolyte and polyvinylidene fluoride (PVDF) or poly-tetra-fluor-ethylene (PTFE) binders, which are highly toxic [4]. The significant dangers posed by the hazardous organic and inorganic materials, especially the fluoride compounds used in the electrolyte and binders, are of major concern to LIB recycling processes' safety [8]. Recycling scrap LIBs therefore provides two main benefits: reducing the impact of waste LIBs on the environment and providing a secondary source for the metals they contain. It has been estimated that recycling LIBs reduces the life cycle impact of LIBs by up to 51% [9].

The continued growth of EVs has led to gradual increases in prices for cobalt, lithium, nickel, and manganese, which are all important metals in the active cathode material. The active cathode material greatly contributes towards the economic feasibility of LIB recycling processes [10] and is recovered to the so-called black mass in the second stage of recycling, following dismantling. The black mass may also contain graphite, organic binders, and parts of the electrodes depending on the dismantling and processing steps of the recycling process [11]. In recent years, the price of lithium carbonate has risen significantly from 4000 USD per metric ton ($/MT) in 2009 [12] to 68,000 $/MT in 2022 [13], with other metals increasing to $75,000 $/MT cobalt [14], $27,000 $/MT nickel [15], and $2300 $/MT manganese in 2022 [16].

1.1. Waste LIB Discharging and Dismantling

The main safety hazard of opening LIBs in air is the exothermic reaction of lithium ions with oxygen, while the safety hazard of opening in water is the generation of explosive hydrogen gas [17]. The use of a NaCl solution to discharge spent LIBs for recycling is the most commonly used conductive solution due to its cost effectiveness, availability, and non-toxicity [18]. Studies have also indicated that increasing the NaCl concentration can increase the discharge rate to allow for faster processing [19].

Discharging LIBs prior to recycling has the added benefit of the intercalation of the Li ions from the anode to the cathode, where Li is thermodynamically stable and does not react violently with water or air [20]. The transfer of the Li ions to the cathode material allows for the maximum recovery of Li to the active cathode powder, leaving the copper anode coated with graphite relatively pure and safe. Most of the lithium is thus recovered with the other high value metals such as cobalt and nickel from the cathode to the black mass. Lithium ions are present in much smaller amounts in the electrolyte and solid electrolyte interface (SEI), which do not pose a safety concern when discharging LIBs, as Li is present as carbonates or fluorides in the SEI and as lithium organic polymers in the electrolyte [21,22].

Punctured and damaged LIB cells can, however, have large deposits of Li in the anode, which, when exposed to air or water, are very reactive [23], and therefore, pyrometallurgical processes that use incineration or complex hydrometallurgical processes that use liquid nitrogen and inert atmospheres are required for safe recycling [11].

The electrolyte poses safety hazards when opening LIBs, as the organic solvent contains lithium salt, typically $LiPF_6$, which hydrolyses in water according to reaction 1 to produce toxic HF gas [24]. The organic solvent typically consists of a mixture of ethylene carbonate and propylene carbonate. Ethylene carbonate is flammable and an irritant of the skin but is classified as non-hazardous for inhalation, while propylene carbonate is flammable and an irritant of the skin, eyes, and lungs [17]. LIBs must therefore be opened in a well-ventilated area, even when fully discharged, to avoid the flammability and toxicity hazards posed by the electrolyte.

$$LiPF_6 + H_2O \rightarrow LiF + POF_3 + 2HF \quad (1)$$

LIBs can vent flammable and toxic gases in the case of overheating, even when thermal runaway is prevented by the deformation of the plastic separator [25,26]. The main safety hazards are due to the possible formation of HF [27] and POF_3 [28] through the decomposition of the $LiPF_6$ salt dissolved in the electrolyte. The fluorine compounds primarily originate from the battery electrolyte but may also originate from the polyvinylidene fluoride (PVDF) or poly-tetra-fluor-ethylene (PTFE) binders in the active electrode materials. $LiPF_6$ decomposes as described in reaction 2 when heated in a dry and inert atmosphere, producing LiF, which is a solid component at temperatures below 845 °C and PF_5 gas [29]. The contact between PF_5 and water will lead to the production of toxic HF and POF_3 according to reaction 3 [29]. Furthermore, contacting POF_3 with water could also lead to the formation of toxic HF with $POF_2(OH)$ according to reaction 4 as suggested by Kawamura et al. [30].

$$LiPF_6 \rightarrow LiF + PF_5 \quad (2)$$

$$PF_5 + H_2O \rightarrow POF_3 + 2HF \quad (3)$$

$$POF_3 + H_2O \rightarrow POF_2(OH) + HF \quad (4)$$

Safely discharging the scrap LIBs in a NaCl solution prevents the fire hazard created when LIB cells short-circuit during cutting or shredding as well as the production of toxic HF gas [31].The internal components of the LIBs can then be sorted to separate the different components, such as the plastic separator, copper anode (coated with carbonaceous material such as graphite), and cathode (coated with active cathode material such as $LiCoO_2$, $LiNi_{1/3}Mn_{1/3}Co_{1/3}O_2$, and $LiFePO_4$). The high value metals of the active cathode material can be further separated prior to recycling by dissolving the Al electrode with an alkaline leach.

The discharging of LIBs in water also poses a safety hazard, as the initial voltage of the LIB cells will be above the electrolysis voltage of water, leading to the production of explosive oxygen and hydrogen gas. To avoid any potential explosive hazards, the discharging process must therefore be performed in a ventilated area such as a fume hood. Discharging batteries to voltages as low as 0 V can lead to irreversible crystal changes of the cathode material, as LIBs are not designed to be operated at such a low voltage [32], leading to significant performance decreases. This is not of concern for LIB recycling processes but may influence processes that aim to regenerate and reuse the cathode material. It has further been illustrated that the energy recovered from scrap LIBs during discharging could provide 7 MJ per ton of batteries, with a 195 Wh/kg energy density and residual charge of 3.0 V [17]. In the case of discharging LIBs with a resistor, the current must be maintained low enough to prevent the batteries from overheating, as the SEI will decompose if the battery temperature exceeds 90 °C [33]. This will lead to the LIB cell shutting down battery function as the plastic separator deforms to prevent the movement of Li ions between the electrodes [26].

1.2. Alkaline Leach of Cathode Electrode

The NaOH alkaline leach selectively targets the aluminium metal present as the cathode current collector, leaving the active cathode powder behind to be recovered as the solid product. The leaching mechanisms of the aluminium current collector and protective layer are illustrated in reaction 5 and 6, respectively [34]. The alkaline leaching of the cathode current collector is a simple and low-cost operation that makes it convenient for large-scale processes. The main consideration with the alkaline leach is the production of hydrogen gas during the leaching of the solid Al metal, as illustrated in reaction 5, and therefore the alkaline leach must be performed in a well-ventilated area to avoid any explosion dangers. A weakness of the NaOH leach is that only the Al current collector will be leached, and therefore, some binders may remain partially attached to the residual active cathode powder.

$$2Al + 2NaOH + 2H_2O \rightarrow 2NaAlO_2 + 3H_2 \quad (5)$$

$$Al_2O_3 + 2NaOH + 3H_2O \rightarrow 2NaAl(OH)_4 \quad (6)$$

Ferreira et al. investigated different NaOH concentrations and observed that increasing the alkali concentration from 1 wt.% to 10 wt.% significantly increased the leaching rate of the current collector [34]. Increasing the concentration of NaOH any further would, however, lead to the formation of a white precipitate with which substantial amounts of Li is lost from the cathode with the Al. The optimum conditions for alkaline leaching of the cathode have been determined to be with a 10 wt.% NaOH solution at 100 g/L for 2 h [4]. The Al-rich leachate produced from the NaOH leach will provide a source of Al, which will aid the economic feasibility of the process; however, the complexities currently faced with alkaline wastewater treatment requires significant considerations for future studies [31].

The recycling of LIBs thus provides notable economic and health benefits but must be performed in the most economically feasible manner that ensures the maximum amount of valuable materials are extracted using a safe process that does not produce large waste streams.

The safety of the discharging and alkaline leach processes to dismantle and recycle LIBs are well-documented throughout literature [11,18,31,34]. These processes enable the safe production of black mass, which is typically the focus of LIB recycling research due to the high economic value presented by the metals such as Co, Ni, Mn, and Li in the active cathode powder [35]. Limited data is, however, available in current literature regarding the efficiency of these processes, specifically the associated metal losses and side streams produced through these processes. In the present study, the LIB discharging and alkaline leach process efficiencies were evaluated. The study focussed on the Al, Co, Li, Mn, and Ni losses from the LIBs throughout these processes and investigates the composition of side streams generated, as illustrated in Figure 1. This will not only aid in better understanding the processes, but also provide insightful data on the potential harmful effects and toxicity of the process streams produced.

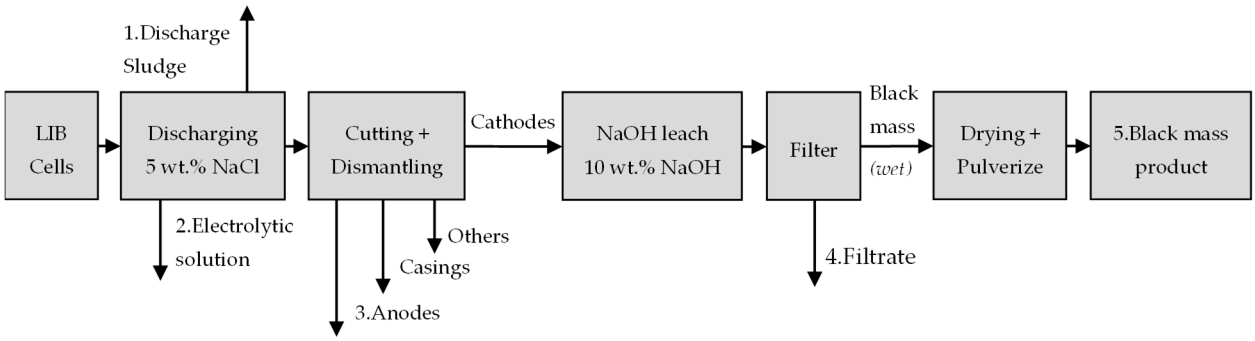

Figure 1. Black mass sample preparation process block flow diagram.

2. Materials and Methods

2.1. Experimental Materials and Reagents

Different types of waste laptop battery packs containing 18,650 cells were used for this study. The LIB discharging was performed with 99 wt.% NaCl supplied by ScienceWorld. The cathodes were leached using 98 wt.% NaOH supplied by Kimix Chemicals and Lab Supplies cc. Aqua regia digestions of the black mass were performed with 60 wt.% HNO_3 and 32.2 wt.% HCl supplied by Kimix Chemicals and Lab Supplies cc. Citric acid leaching was performed with 99.8 wt.% anhydrous citric acid powder and 50 wt.% H_2O_2 supplied by Kimix Chemicals and Lab Supplies cc. Demineralised water was used for the dilution of all reagents in this study.

2.2. Equipment

The laptop battery packs were dismantled manually with pliers and a screwdriver to obtain the individual cells. The LIB cells were discharged in an open glass beaker placed in a fume hood after which the LIB cells were air dried on paper towels. The discharge sludge was separated from the electrolytic solution using a vacuum filter. The dried cells were tested with a multimeter to determine their voltage, and the casings were cut with a bandsaw. The casings were bent open with a screwdriver and the cathode strips were then treated with NaOH in an open 5 L vessel fitted with an overhead stirrer, inside a fume hood.

2.3. Experimental Procedure

Each LIB cell was measured with a digital multimeter after dismantling to determine if the cells contained any residual charge, which may pose a threat during cutting. All the LIBs with a voltage of under 0.5 V were deemed safe for cutting; however, the LIBs with a residual charge greater than 0.5 V were deemed unsafe to cut open and were therefore treated prior to cutting.

The LIBs with a residual charge greater than 0.5 V were discharged in a 5 wt.% NaCl solution, prepared with demineralised water, for 48 h at 22 ± 3 °C to allow them to be cut open safely [36]. After the 48 h discharging, the LIB cells were allowed to air dry, and the

electrolytic solution was separated from the discharge sludge formed by using a vacuum filter. The batteries were then again checked with a multimeter to ensure that their voltage was below 0.5 V before cutting them open with a bandsaw to recover the electrode coil.

The electrode coils were then unravelled, and the LIB components were manually dismantled and sorted into groups. The cathode electrodes were cut into smaller 2 cm by 2 cm pieces using a pair of scissors and sent for further treatment. The aluminium cathode electrode was leached with 10 wt.% NaOH, using a pulp density of 100 g/L for 2 h at room temperature in a fume hood, allowing the separation of the protective layer (Al_2O_3) and active cathode powder from the aluminium solution by filtration [37]. After the black mass was air dried, it was pulverised into a fine powder for leaching. Five aqua regia digestions were completed to characterise the metal composition of the black mass at 60 °C and pulp density of 50 g/L for 48 h.

All liquid samples were analysed with a Perkin Elmer Avio 500 ICP-OES. The solid samples were analysed with a Carl Zeiss Merlin Field Emission Scanning Electron Microscope (FESEM) with an Energy Dispersive Spectroscopy (EDS) attachment. The metal phases were analysed with a PANalytical Aeris benchtop diffractometer (Malvern Panalytical, Malvern, UK) with a PIXcel1D detector (Malvern Panalytical, Malvern, UK) and fixed slits with iron filtered Co-Kα radiation. The phases were identified using X'Pert Highscore plus software version 4.8, and the relative phase amounts in the black mass were quantified by weight percentage using the Rietveld method.

3. Results and Discussion

3.1. Discharging

The LIBs with a residual charge greater than 0.5 V were discharged in a 5 wt.% NaCl solution, where 250 g LIB cells could be successfully discharged in a 1 L working volume within 48 h. During the first 12 h of the discharging, it was observed that a sludge formed on top of the electrolytic solution in the beaker as the LIB cells produced small bubbles while they discharged. This sludge is referred to as the discharge sludge throughout this study. These bubbles have previously been reported to be a combination of hydrogen and oxygen as the initial voltage of the cells exceeds the electrolysis voltage of water [17]. The discharging was thus performed in a fume hood to avoid any potential flammable or explosion dangers.

The discharge sludge was separated by vacuum filtration after the discharging process and was allowed to air dry before a FESEM-EDS analysis. Typical results are illustrated in Figure 2. It was observed that the discharge sludge composition consisted of a mixture of 34.9 wt.% Fe, 17.7 wt.% Al, 6.2 wt.% C, 4.2 wt.% Na, and 35.0 wt.% O. The blue particles were identified as NaCl, and small yellow spots on the discharge spots were determined to consist of 55 wt.% Fe, 8 wt.% Al, 4 wt.% Na, 3.6 wt.% C, and 28 wt.% O.

Table 1 summarises the metal fraction reporting to the discharge sludge and electrolytic solution, respectively, from the LIBs during the discharging process. The most significant losses were observed to be 89.4% Fe, 3.0% Cu, and 1.9% Al, which all report to the discharge sludge. It is theorised that this is due to the electrochemical cell created in the electrolytic solution with the residual electric potential in the LIBs, which corroded the cell casings, as the cell casings were observed to be heavily corroded during the discharging process.

Table 1 further illustrates the limited amount of metals reporting to the electrolytic solution, indicating that the electrolytic solution can potentially be reused for multiple cycles. The amount of cathode metals reporting to the discharging side streams from the LIBs in Table 1 was greatly limited to 0.01% Co, 0.01% Li, 0.01% Mn, and 0.02% Ni. The discharging process thus shows great promise, as these metals will be targeted by recycling the black mass downstream, which typically drives the economic feasibility of the recycling process due to the high value metals.

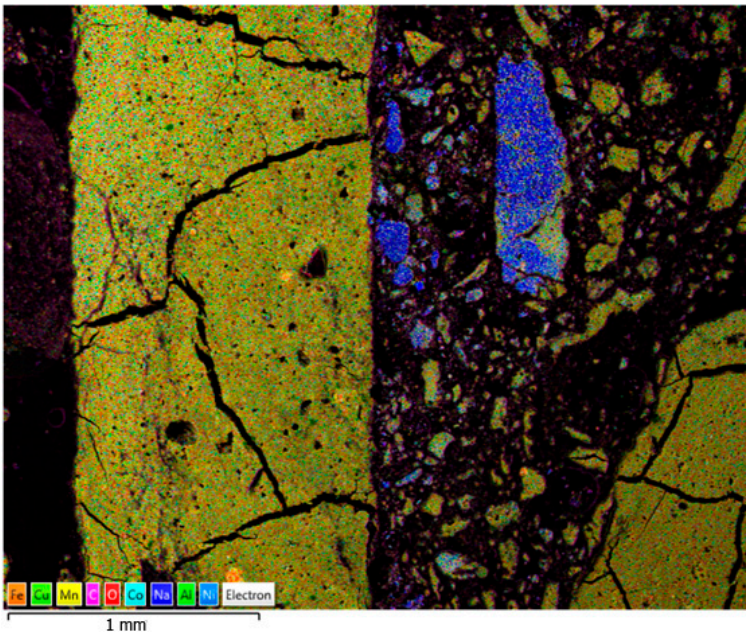

Figure 2. Field Emission Scanning Electron Microscope with Energy Dispersive Spectroscopy (FESEM-EDS) layered map for discharge residue.

Table 1. Percentage of metals in the feed reporting to the LIB discharging side streams.

Discharge Stream	Stream	Al	Co	Cu	Fe	Li	Mn	Ni
Discharge sludge	1	1.93%	0.01%	2.98%	89.37%	-	0.01%	0.02%
Electrolytic solution	2	0.00%	0.00%	0.00%	0.34%	0.01%	0.00%	0.00%

Table 2 summarises the average metal composition of the discharge sludge and the electrolytic solution and confirms the limited amount of cathodic metals reporting to the LIB discharging process side streams. The electrolytic solution contains 12.6 mg/L Fe, 4.5 mg/L Li, 2.5 mg/L Mn, 1 mg/L Ni, and trace amounts of Co. Due to the dilute metals present in this stream, the electrolytic solution could potentially be reused for subsequent discharging cycles before being treated to recover the metals it contains.

Table 2. Average discharge sludge and electrolytic solution metal composition.

Discharge Stream	Stream	Al	Co	Cu	Fe	Li	Mn	Ni
Discharge sludge (wt.%)	1	17.99%	0.21%	0.11%	39.09%	-	0.12%	0.35%
Electrolytic solution (mg/L)	2	0.0000	0.7177	0.0000	12.62	4.504	2.554	1.012

The small quantities of lithium in the electrolytic solution originate from either the anode, where Li ions are stored when charged, or from the electrolyte, which contains $LiPF_6$. It is, however, known that $LiPF_6$ decomposes in water to form LiF, which is solid at temperatures under 845 °C and has a low solubility in water [38]. The low solubility of LiF in water could be responsible for the dilute quantities of Li reporting to the electrolytic solution. The presence of Li could not be detected with the SEM-EDS analysis due to its low energy of characteristic radiation, but no fluoride was detected within the discharge sludge residue. It is therefore theorised that no Li reports to the discharge sludge as LiF.

The average composition of the discharge sludge in Table 2 clearly illustrates that the main components of the sludge are 39.1 wt.% Fe and 18.0 wt.% Al. The other major components of the sludge were quantified with the SEM-EDS analysis and include 30.1 wt.% O, 6.6 wt.% Na, and 4.4 wt.% C. The discharge sludge could thus provide a secondary source for Fe and Al once dried to be reused in a circular economy.

After the batteries were all discharged to under 0.5 V, they were deemed to be safe and were manually cut open using a bandsaw. As illustrated in Table 3, the cathode accounted for nearly 29.75% of the LIBs by weight, while the anode accounted for 19.58% and the casings 21.56%. The plastic separators, plastic wrapping, centre pins, vent disks, and other materials not part of the electrodes accounted for 29.11% and were labelled as others.

Table 3. LIB component weight fractions.

Component	Cathode	Anode	Others [1]	Casings
Weight %	29.75%	19.58%	29.11%	21.56%

[1] Plastic separator and all materials inside the LIBs, which are not part of the electrodes.

3.2. NaOH Leaching of Cathode Material

The separation of the active cathode material was targeted next, by selectively leaching the aluminium cathode electrode with an alkaline leach, to produce a relatively pure black mass. The black mass residue containing active cathode powder can then subsequently be used to recover the desired high value metals. It was thus required to minimise the losses of cathode metals to the NaOH leach filtrate to ensure high metal recoveries to the black mass product.

Table 4 summarises the metals reporting to the process streams investigated in this study. It was observed in Table 4 that more than 90% of the Al was recovered to the NaOH leach filtrate. It was also observed that 3.2% of the Cu was recovered to the NaOH leach filtrate, which originates from the anode electrode, indicating some slight contamination of the anode in the black mass due to imperfect sorting. It was further observed that nearly 94% of the Cu was recovered to the solid anodes during the LIB component sorting. The NaOH leach filtrate was highly selective for the aluminium electrode over the active cathode material, as only 0.04% Co, 0.19% Li, and 0.01% Mn reported to the NaOH leach filtrate from the active cathode material. The balance of all the metals reported to the black mass product.

Table 4. Percentage of the metals reporting to the process streams from the LIB feed.

Process Stream	Stream	Al	Co	Cu	Fe	Li	Mn	Ni
Discharging side streams	1 + 2	1.93%	0.01%	2.98%	89.71%	0.01%	0.01%	0.02%
NaOH leach filtrate	4	90.54%	0.04%	3.16%	0.00%	0.19%	0.01%	0.00%
Anodes	3	0.00%	0.00%	93.86%	0.00%	0.00%	0.00%	0.00%
Black mass product	5	7.53%	99.95%	0.00%	10.29%	99.80%	99.98%	99.98%

Ferreira et al. suggested that the leaching of lithium observed during the NaOH leaching could originate from the lithium metal oxide phases (active cathode material) or the electrolyte [34]. The lithium metal oxide phases could be dissolved to some extent when the lithium is extracted, as it is known that metals such as cobalt can form stable solid complexes in the form of Co_3O_4 and $Co(OH)_2$. The lithium ions would then react exothermically with the water to produce hydrogen gas and LiOH, which is very soluble in water [39]. The lithium could also originate from the dissolution of the $LiPF_6$ electrolyte. It is, however, unlikely that the lithium originated from the decomposition or hydrolysis of the $LiPF_6$ electrolyte, as this would lead to the decomposition of the $LiPF_6$, as illustrated in reactions 1 to 4, and no fluoride compounds were detected in the discharge residue.

Table 4 illustrates that the discharging and NaOH leach processes performed favourably, resulting in high metal recoveries to the black mass product. The limited amounts of Co, Li, Mn, and Ni, which all originate from the active cathode powder, reporting to the discharge and NaOH leach streams confirm the effectiveness of the processes to produce a highly pure black mass containing mostly active cathode material with minimal losses of high value metals.

Table 5 summarises the composition of the NaOH leach filtrate, and it is clear that the leach stream is rich in Al, with a concentration of roughly 9558 mg/L Al. It is thus highly recommended that future studies investigate the recovery of Al from the NaOH leach filtrate through further processing, as this could provide a significant secondary source of Al. The filtrate also contains dilute quantities of the valuable active cathode materials, with around 13.2 mg/L Li, 8.7 mg/L Co, 1.6 mg/L Mn, and 0.5 mg/L Ni. The dilute quantity of Ni detected with ICP-OES in the NaOH leach in Table 5 is not reflected in Table 4, as the minor amount of Ni reporting to the NaOH leach filtrate accounts for 0.003% of the total Ni in the LIB feed. Furthermore, the Cu concentration in the NaOH leach filtrate is very low in comparison to Co, even though it had a higher leaching recovery. This is due to Cu being present in smaller quantities in the NaOH leach feed compared to the metals such as Co, Li, Mn, and Ni, which are more concentrated in the cathode.

Table 5. NaOH leach filtrate metal composition.

Process Stream	Al	Co	Cu	Fe	Li	Mn	Ni
NaOH leach filtrate (mg/L)	9558	8.665	1.802	0.000	13.15	1.594	0.5153

The solid residue separated during the filtering of the NaOH leach filtrate was washed with demineralised water and allowed to air dry, after which the residue was pulverised into a fine powder. This powder, also known as black mass, contains the high value metals in the form of the active cathode powder. The black mass was thus characterised with various different analytical techniques to gain further knowledge into the effectiveness of the discharging and NaOH leach processes, as well as the composition and structure of the black mass.

3.3. Black Mass Characterisation

The crystalline phases of the black mass powder were characterised with X-ray powder diffraction (XRD) analysis, and it was determined that the metal phase consists of 15.8% $LiCoO_2$ (LCO) and 84.2% $LiNi_xMn_yCo_zO_2$ (NMC), as illustrated in Figure 3. Any amorphous phases were not considered during quantification, and the phase names may not reflect the actual compositions of phases identified, but the phase group. A few small peaks could not be matched, and trace amounts of additional phases may thus be present, as phases below 3 wt.% were below the detection limit and not included.

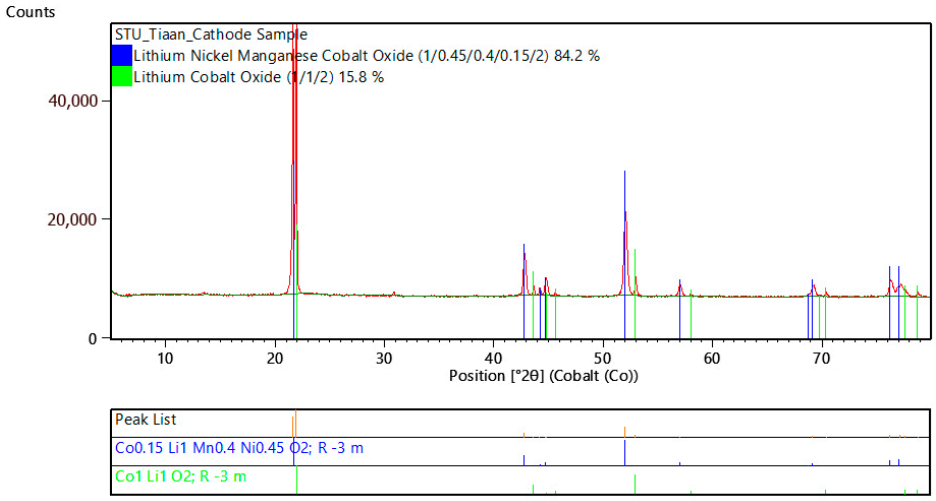

Figure 3. XRD analysis of the black mass powder.

The FESEM-EDS analysis of the black mass illustrated in Figure 4 shows definitive phase segregation between the different cathodic materials originating from the different

waste LIBs. The distinctly different phases were analysed at the chosen spectrums illustrated in Figure A1. The weight percentages of each metal in the spectrums were measured, as summarised in Table A1, and converted to molar fractions in Table A2 to determine the metal content for each phase, which led to the identification of three distinct cathodic phases:

1. Large blue particles—CoO_2 (LCO);
2. Fine light-yellow particles—$Ni_xMn_yCo_zO_2$ (NMC);
3. Fine dark-yellow particles—Mn_2O_4 (LMO)

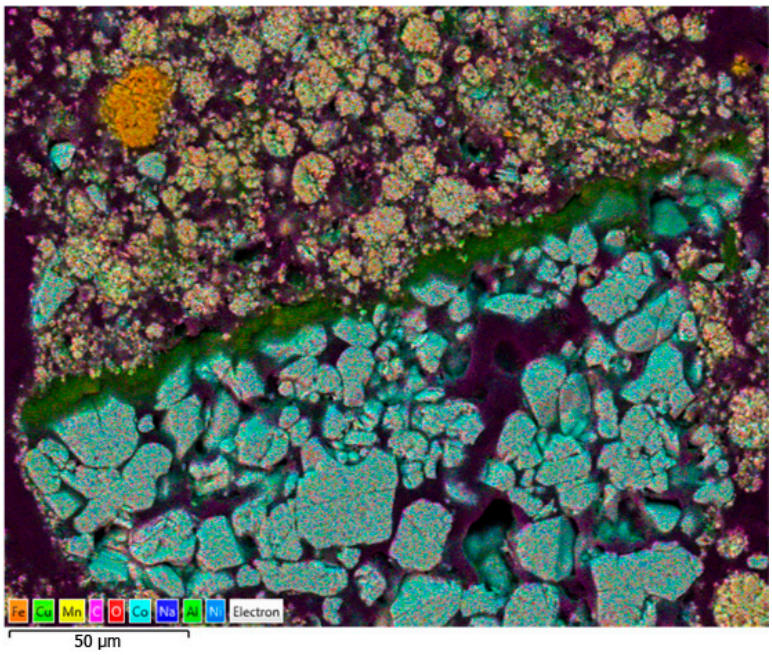

Figure 4. FESEM-EDS layered image of black mass powder sample.

The LMO was not detected during the XRD analysis due to the small fraction of LMO material present in the black mass being lower than the detection limit of the XRD analysis (3 wt.%). It was further observed that a green barrier phase was present in multiple samples near the LCO phase, which was identified as the protective aluminium oxide layer (Al_2O_3) located between the aluminium cathode film and the active cathodic material [4]. It is unclear why the Al_2O_3 layer is only associated with the LCO phases investigated, and not the NMC or LMO phases observed, but might be due to manufacturing specifications and specific organic binder selections. It is recommended that future studies investigate the removal of the Al_2O_3 layer with higher NaOH concentrations and higher leach temperatures, as the Eh-pH diagrams for the Al-Na-H_2O system indicates increased stability of the aqueous $Na[Al(OH)_4]$ complex when these variables are increased [34].

No fluoride components were identified in the FESEM-EDS analysis of the black mass, indicating that the organic binders (PVDF, PTFE) and electrolyte salts ($LiPF_5$) were not present in the black mass produced. It is therefore theorised that the binders and electrolyte were dissolved or broken down in the discharging process or strong alkaline leach.

The average metal composition of the black mass was determined with aqua regia digestions and is summarised in Table 6. It was observed that Co, Ni, and Mn are the major metals present in the black mass. Trace amounts of Al were also detected, which originate from the Al_2O_3 layer identified in the FESEM-EDS analysis. The mass fraction of lithium is comparatively low compared with the other metals because it has a much smaller molar mass; however, lithium accounts for 48% of the molar fraction of the cathode powder and remains the essential element for LIB performance due to its high charge to weight ratio and high specific heat capacity [3].

Table 6. The average metal content and standard error of LIB black mass powder.

Process Stream	Al		Co		Li		Mn		Ni	
Black mass (wt.%)	1.2%	±0.0%	35.4%	±1.4%	10.2%	±0.4%	23.4%	±0.9%	29.7%	±1.2%

The black mass produced in this study provides a highly pure stream of active cathode material through a process that uses easily accessible chemicals, no heating, and safe operating conditions. The black mass is used as feed material for recycling processes that typically focus on the separation and recovery of Co, Li, Ni, and Mn due to the significant economic benefit they provide. The high purity black mass is an ideal feed for hydrometallurgical processes, which are considered to be the most promising method for LIB recycling due to their high metal extraction, metal product purity, low energy consumption, and reduced gas emissions [40]. The effective separation of the active cathode material during sample preparation reduces the number of metals in the feed material, producing a simpler lixiviant with less potential for variation, which is desired, as hydrometallurgical processes are sensitive to changes in the process input [41].

Hydrometallurgical LIB recycling processes have been researched extensively, especially for processes using H_2SO_4 [42–46] and HCl [47–52] as lixiviants. Recent research has further investigated the potential use of citric acid as lixiviant [53,54], which has shown high leaching performance [35,51,55–57] and unique metal separation opportunities due to the chelating properties of citric acid [58,59]. Metal separation and recovery processes typically make use of solvent extraction and precipitation techniques, depending on the metal content of the leach solution, to produce metal products that can be reused for battery manufacturing if the product is of sufficient quality [60].

4. Conclusions

Discharging of the LIBs in a 5 wt.% NaCl solution produced a sludge containing metals originating from the cell casings, metal electrodes, and NaCl from the electrolytic solution. It was concluded that the electrolytic solution contained trace amounts of metals, where 0.3% Fe from the LIBs reported to the electrolytic solution with <0.01% of all the other metals. The electrolytic solution could thus be reused for further discharging cycles before being treated or purged. The composition of the electrolytic solution comprised of 12.6 mg/L Fe, 4.5 mg/L Li, 2.6 mg/L Mn, 1.0 mg/L Ni, and 0.7 mg/L Co.

The discharge sludge contained aluminium, iron, and oxygen with traces of carbon. An analysis illustrated that 1.9% Al, 3.0% Cu, and 89.4% Fe reported to the discharge sludge from the waste LIBs and that the composition of the discharge sludge consisted of 39.1 wt.% Fe, 30.1 wt.% O, 18.0 wt.% Al, 6.6 wt.% Na, and 4.4 wt.% C. Limited metals from the active cathode material reported to the discharge sludge, as 0.01% Co, 0.01% Mn, and 0.02% Ni reported to the sludge from the LIBs.

The cathode electrodes sorted from the cut LIBs accounted for 29.75% of the LIB weight and was recovered after the LIB discharging. A 10 wt.% NaOH leach successfully dissolved the aluminium electrode, enabling the separation of the active cathode material. This study concluded that 90.5% Al and 3.2% Cu is recovered to the NaOH leach filtrate with 0.04% Co, 0.19% Li, and 0.01% Mn. The NaOH leach filtrate provides a rich secondary source of Al, as the filtrate contained 9 558 mg/L Al with trace amounts of other metals, including: 13.2 mg/L Li, 8.7 mg/L Co, 1.8 mg/L Cu, 1.6 mg/L Mn, and 0.5 mg/L Ni.

Characterisation of the black mass produced through discharging, dismantling, sorting, and alkaline leach processes confirmed the high active cathode material purity of the black mass. XRD analysis confirmed the crystalline phases as 84.2 wt.% $LiNi_xMn_yCo_zO_2$ and 15.8 wt.% $LiCoO_2$. A SEM-EDS analysis confirmed the crystalline phases, with trace amounts of MnO_2 also identified. The presence of an Al_2O_3 layer was also observed around some LCO phases, indicating the inability of the alkaline leach to completely remove the protective layer (Al_2O_3) located between the cathode electrode and active material. The organic binders were not detected in the characterisation of the black mass, and therefore,

the alkaline leach may have dissolved or broken down the binders during the alkaline leach process.

The sample preparation process effectively produced a highly pure black mass, with minimal Co, Li, Mn, and Ni losses from the high value active cathode material to the discharging and NaOH leach streams. The ability of these processes to operate at room temperature with simple operating conditions, and readily available chemicals makes them an ideal candidate for preparing black mass from spent LIBs for hydrometallurgical recycling processes.

Author Contributions: Conceptualisation, T.P.; methodology, T.P.; validation, P.v.W., S.M.B. and G.A.; formal analysis, T.P.; investigation, T.P.; data curation, P.v.W. and G.A.; writing—original draft preparation, T.P.; writing—review and editing, S.M.B., P.v.W. and G.A.; supervision, P.v.W. and S.M.B.; project administration, G.A.; funding acquisition, S.M.B. and G.A. All authors have read and agreed to the published version of the manuscript.

Funding: This research received no external funding.

Data Availability Statement: The data presented in this study are available on request from the corresponding author.

Acknowledgments: The authors would like to thank the Wilhelm Frank Trust and the Stellenbosch University Postgraduate Scholarship Programme for supporting this research project.

Conflicts of Interest: The authors declare no conflict of interest.

Appendix A

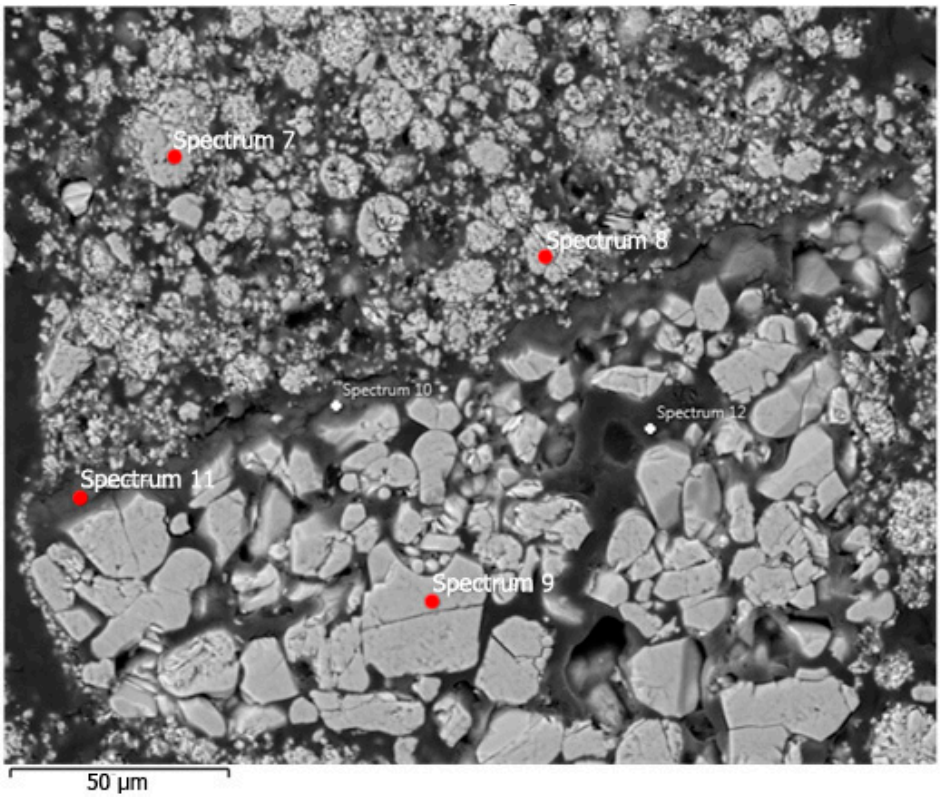

Figure A1. Spectrum locations identified for phase composition analysis.

Table A1. Metal weight percentage of identified spectrums.

Spectrum	C	O	Na	Al	Mn	Fe	Co	Ni	Cu	Total
Spectrum 7	2.0%	37.2%	0.2%	0.1%	59.2%	0.0%	0.7%	0.5%	0.1%	100.0%
Spectrum 8	1.8%	29.8%	0.2%	0.1%	18.6%	0.2%	15.5%	33.7%	0.2%	100.0%
Spectrum 9	1.5%	33.0%	0.0%	0.0%	0.4%	0.0%	65.0%	0.1%	0.0%	100.0%
Spectrum 11	14.8%	41.9%	0.0%	20.6%	0.5%	0.2%	21.7%	0.4%	0.1%	100.0%

Table A2. Metal molar fractions of identified spectrums.

Spectrum	C	O	Na	Al	Mn	Fe	Co	Ni	Cu	Total
Spectrum 7	4.5%	64.6%	0.2%	0.1%	30.0%	0.0%	0.3%	0.3%	0.0%	100.0%
Spectrum 8	4.7%	58.0%	0.3%	0.1%	10.6%	0.1%	8.2%	17.9%	0.1%	100.0%
Spectrum 9	3.8%	62.5%	0.0%	0.0%	0.2%	0.0%	33.4%	0.1%	0.0%	100.0%
Spectrum 11	24.6%	52.4%	0.0%	15.2%	0.2%	0.1%	7.4%	0.1%	0.0%	100.0%

References

1. Nishi, Y. Past, Present and Future of Lithium-Ion Batteries: Can New Technologies Open up New Horizons? In *Lithium-Ion Batteries: Advances and Applications*; Pistoia, G., Ed.; Elsevier: Amsterdam, The Netherlands, 2014; pp. 21–39; ISBN 9780444595133.
2. Choubey, P.K.; Chung, K.-S.; Kim, M.; Lee, J.; Srivastava, R.R. Advance Review on the Exploitation of the Prominent Energy-Storage Element Lithium. Part II: From Sea Water and Spent Lithium Ion Batteries (LIBs). *Miner. Eng.* **2017**, *110*, 104–121. [CrossRef]
3. Swain, B. Recovery and Recycling of Lithium: A Review. *Sep. Purif. Technol.* **2017**, *172*, 388–403. [CrossRef]
4. Zheng, X.; Zhu, Z.; Lin, X.; Zhang, Y.; He, Y.; Cao, H.; Sun, Z. A Mini-Review on Metal Recycling from Spent Lithium Ion Batteries. *Engineering* **2018**, *4*, 361–370. [CrossRef]
5. Natarajan, S.; Aravindan, V. Burgeoning Prospects of Spent Lithium-Ion Batteries in Multifarious Applications. *Adv. Energy Mater.* **2018**, *8*, 1802303. [CrossRef]
6. Zhao, S.; He, W.; Li, G. Recycling Technology and Principle of Spent Lithium-Ion Battery. In *Recycling of Spent Lithium-Ion Batteries*; Springer International Publishing: Cham, Switzerland, 2019; pp. 1–26.
7. Kang, D.H.P.; Chen, M.; Ogunseitan, O.A. Potential Environmental and Human Health Impacts of Rechargeable Lithium Batteries in Electronic Waste. *Environ. Sci. Technol.* **2013**, *47*, 5495–5503. [CrossRef]
8. Zhang, G.; Du, Z.; He, Y.; Wang, H.; Xie, W.; Zhang, T. A Sustainable Process for the Recovery of Anode and Cathode Materials Derived from Spent Lithium-Ion Batteries. *Sustainability* **2019**, *11*, 2363. [CrossRef]
9. Wang, X.; Gaustad, G.; Babbitt, C.W.; Richa, K. Economies of Scale for Future Lithium-Ion Battery Recycling Infrastructure. *Resour. Conserv. Recycl.* **2014**, *83*, 53–62. [CrossRef]
10. Rinne, M.; Elomaa, H.; Porvali, A.; Lundström, M. Simulation-Based Life Cycle Assessment for Hydrometallurgical Recycling of Mixed LIB and NiMH Waste. *Resour. Conserv. Recycl.* **2021**, *170*, 105586. [CrossRef]
11. Winslow, K.M.; Laux, S.J.; Townsend, T.G. A Review on the Growing Concern and Potential Management Strategies of Waste Lithium-Ion Batteries. *Resour. Conserv. Recycl.* **2018**, *129*, 263–277. [CrossRef]
12. Ali, H.; Khan, H.A.; Pecht, M.G. Circular Economy of Li Batteries: Technologies and Trends. *J. Energy Storage* **2021**, *40*, 102690. [CrossRef]
13. Trading Economics Lithium Commodity Price. Available online: https://tradingeconomics.com/commodity/lithium (accessed on 27 May 2022).
14. Trading Economics Cobalt Commodity Price. Available online: https://tradingeconomics.com/commodity/cobalt (accessed on 27 May 2022).
15. Trading Economics Nickel Commodity Price. Available online: https://tradingeconomics.com/commodity/nickel (accessed on 27 May 2022).
16. Shanghai Metal Market (SMM) Manganese Commodity Price. Available online: https://price.metal.com/Manganese (accessed on 27 May 2022).
17. Sonoc, A.; Jeswiet, J.; Soo, V.K. Opportunities to Improve Recycling of Automotive Lithium Ion Batteries. *Procedia CIRP* **2015**, *29*, 752–757. [CrossRef]
18. Yu, D.; Huang, Z.; Makuza, B.; Guo, X.; Tian, Q. Pretreatment Options for the Recycling of Spent Lithium-Ion Batteries: A Comprehensive Review. *Miner. Eng.* **2021**, *173*, 107218. [CrossRef]
19. Li, J.; Wang, G.; Xu, Z. Generation and Detection of Metal Ions and Volatile Organic Compounds (VOCs) Emissions from the Pretreatment Processes for Recycling Spent Lithium-Ion Batteries. *Waste Manag.* **2016**, *52*, 221–227. [CrossRef] [PubMed]
20. Park, J.-K. *Principles and Applications of Lithium Secondary Batteries*; Wiley-VCH Verlag GmbH & Co. KGaA: Weinheim, Germany, 2012; ISBN 978-3-527-33151-2.

21. Gratz, E.; Sa, Q.; Apelian, D.; Wang, Y. A Closed Loop Process for Recycling Spent Lithium Ion Batteries. *J. Power Sources* **2014**, *262*, 255–262. [CrossRef]
22. Ra, D.; Han, K.-S. Used Lithium Ion Rechargeable Battery Recycling Using Etoile-Rebatt Technology. *J. Power Sources* **2006**, *163*, 284–288. [CrossRef]
23. Vetter, J.; Novák, P.; Wagner, M.R.; Veit, C.; Möller, K.-C.; Besenhard, J.O.; Winter, M.; Wohlfahrt-Mehrens, M.; Vogler, C.; Hammouche, A. Ageing Mechanisms in Lithium-Ion Batteries. *J. Power Sources* **2005**, *147*, 269–281. [CrossRef]
24. Vikström, H.; Davidsson, S.; Höök, M. Lithium Availability and Future Production Outlooks. *Appl. Energy* **2013**, *110*, 252–266. [CrossRef]
25. Zhang, Z.J.; Ramadass, P.; Fang, W. Safety of Lithium-Ion Batteries. In *Lithium-Ion Batteries*; Elsevier: Amsterdam, The Netherlands, 2014; pp. 409–435.
26. Doughty, D.H.; Roth, E.P. A General Discussion of Li Ion Battery Safety. *Electrochem. Soc. Interface* **2012**, *21*, 37–44. [CrossRef]
27. NIOSH. Documentation for Immediately Dangerous to Life or Health Concentrations (IDLHs) for Hydrogen Fluoride—The National Institute for Occupational Safety and Health. Available online: https://www.cdc.gov/niosh/idlh/7664393.html (accessed on 7 February 2022).
28. Larsson, F.; Andersson, P.; Blomqvist, P.; Lorén, A.; Mellander, B.-E. Characteristics of Lithium-Ion Batteries during Fire Tests. *J. Power Sources* **2014**, *271*, 414–420. [CrossRef]
29. Yang, H.; Zhuang, G.V.; Ross, P.N. Thermal Stability of LiPF6 Salt and Li-Ion Battery Electrolytes Containing LiPF6. *J. Power Sources* **2006**, *161*, 573–579. [CrossRef]
30. Kawamura, T.; Okada, S.; Yamaki, J. Decomposition Reaction of LiPF6-Based Electrolytes for Lithium Ion Cells. *J. Power Sources* **2006**, *156*, 547–554. [CrossRef]
31. Raj, T.; Chandrasekhar, K.; Kumar, A.N.; Sharma, P.; Pandey, A.; Jang, M.; Jeon, B.-H.; Varjani, S.; Kim, S.-H. Recycling of Cathode Material from Spent Lithium-Ion Batteries: Challenges and Future Perspectives. *J. Hazard. Mater.* **2022**, *429*, 128312. [CrossRef] [PubMed]
32. Shu, J.; Shui, M.; Xu, D.; Wang, D.; Ren, Y.; Gao, S. A Comparative Study of Overdischarge Behaviors of Cathode Materials for Lithium-Ion Batteries. *J. Solid State Electrochem.* **2012**, *16*, 819–824. [CrossRef]
33. Lu, L.; Han, X.; Li, J.; Hua, J.; Ouyang, M. A Review on the Key Issues for Lithium-Ion Battery Management in Electric Vehicles. *J. Power Sources* **2013**, *226*, 272–288. [CrossRef]
34. Ferreira, D.A.; Prados, L.M.Z.; Majuste, D.; Mansur, M.B. Hydrometallurgical Separation of Aluminium, Cobalt, Copper and Lithium from Spent Li-Ion Batteries. *J. Power Sources* **2009**, *187*, 238–246. [CrossRef]
35. Meng, F.; Liu, Q.; Kim, R.; Wang, J.; Liu, G.; Ghahreman, A. Selective Recovery of Valuable Metals from Industrial Waste Lithium-Ion Batteries Using Citric Acid under Reductive Conditions: Leaching Optimization and Kinetic Analysis. *Hydrometallurgy* **2020**, *191*, 105160. [CrossRef]
36. He, L.-P.; Sun, S.-Y.; Mu, Y.-Y.; Song, X.-F.; Yu, J.-G. Recovery of Lithium, Nickel, Cobalt, and Manganese from Spent Lithium-Ion Batteries Using l -Tartaric Acid as a Leachant. *ACS Sustain. Chem. Eng.* **2017**, *5*, 714–721. [CrossRef]
37. Li, L.; Fan, E.; Guan, Y.; Zhang, X.; Xue, Q.; Wei, L.; Wu, F.; Chen, R. Sustainable Recovery of Cathode Materials from Spent Lithium-Ion Batteries Using Lactic Acid Leaching System. *ACS Sustain. Chem. Eng.* **2017**, *5*, 5224–5233. [CrossRef]
38. Stubblefield, C.B.; Bach, R.O. Solubility of Lithium Fluoride in Water. *J. Chem. Eng. Data* **1972**, *17*, 491–492. [CrossRef]
39. Klanchar, M.; Wintrode, B.D.; Phillips, J.A. Lithium−Water Reaction Chemistry at Elevated Temperature. *Energy Fuels* **1997**, *11*, 931–935. [CrossRef]
40. Lie, J.; Liu, J.-C. Closed-Vessel Microwave Leaching of Valuable Metals from Spent Lithium-Ion Batteries (LIBs) Using Dual-Function Leaching Agent: Ascorbic Acid. *Sep. Purif. Technol.* **2021**, *266*, 118458. [CrossRef]
41. Huang, B.; Pan, Z.; Su, X.; An, L. Recycling of Lithium-Ion Batteries: Recent Advances and Perspectives. *J. Power Sources* **2018**, *399*, 274–286. [CrossRef]
42. Swain, B.; Jeong, J.; Lee, J.; Lee, G. Separation of Cobalt and Lithium from Mixed Sulphate Solution Using Na-Cyanex 272. *Hydrometallurgy* **2006**, *84*, 130–138. [CrossRef]
43. Chen, L.; Tang, X.; Zhang, Y.; Li, L.; Zeng, Z.; Zhang, Y. Process for the Recovery of Cobalt Oxalate from Spent Lithium-Ion Batteries. *Hydrometallurgy* **2011**, *108*, 80–86. [CrossRef]
44. Zhao, J.M.; Shen, X.Y.; Deng, F.L.; Wang, F.C.; Wu, Y.; Liu, H.Z. Synergistic Extraction and Separation of Valuable Metals from Waste Cathodic Material of Lithium Ion Batteries Using Cyanex272 and PC-88A. *Sep. Purif. Technol.* **2011**, *78*, 345–351. [CrossRef]
45. Dorella, G.; Mansur, M.B. A Study of the Separation of Cobalt from Spent Li-Ion Battery Residues. *J. Power Sources* **2007**, *170*, 210–215. [CrossRef]
46. Choubey, P.K.; Dinkar, O.S.; Panda, R.; Kumari, A.; Jha, M.K.; Pathak, D.D. Selective Extraction and Separation of Li, Co and Mn from Leach Liquor of Discarded Lithium Ion Batteries (LIBs). *Waste Manag.* **2021**, *121*, 452–457. [CrossRef]
47. Torkaman, R.; Asadollahzadeh, M.; Torab-Mostaedi, M.; Maragheh, M.G. Recovery of Cobalt from Spent Lithium Ion Batteries by Using Acidic and Basic Extractants in Solvent Extraction Process. *Sep. Purif. Technol.* **2017**, *186*, 318–325. [CrossRef]
48. Song, Y.; Zhao, Z.; He, L. Lithium Recovery from Li3PO4 Leaching Liquor: Solvent Extraction Mechanism of Saponified D2EHPA System. *Sep. Purif. Technol.* **2020**, *249*, 117161. [CrossRef]
49. Contestabile, M.; Panero, S.; Scrosati, B. A Laboratory-Scale Lithium Ion Battery Recycling Process. *J. Power* **2001**, *92*, 65–69. [CrossRef]

50. Joulié, M.; Laucournet, R.; Billy, E. Hydrometallurgical Process for the Recovery of High Value Metals from Spent Lithium Nickel Cobalt Aluminum Oxide Based Lithium-Ion Batteries. *J. Power Sources* **2014**, *247*, 551–555. [CrossRef]
51. Li, L.; Zhai, L.; Zhang, X.; Lu, J.; Chen, R.; Wu, F.; Amine, K. Recovery of Valuable Metals from Spent Lithium-Ion Batteries by Ultrasonic-Assisted Leaching Process. *J. Power Sources* **2014**, *262*, 380–385. [CrossRef]
52. Wesselborg, T.; Virolainen, S.; Sainio, T. Recovery of Lithium from Leach Solutions of Battery Waste Using Direct Solvent Extraction with TBP and FeCl3. *Hydrometallurgy* **2021**, *202*, 105593. [CrossRef]
53. Golmohammadzadeh, R.; Faraji, F.; Rashchi, F. Recovery of Lithium and Cobalt from Spent Lithium Ion Batteries (LIBs) Using Organic Acids as Leaching Reagents: A Review. *Resour. Conserv. Recycl.* **2018**, *136*, 418–435. [CrossRef]
54. Yu, M.; Zhang, Z.; Xue, F.; Yang, B.; Guo, G.; Qiu, J. A More Simple and Efficient Process for Recovery of Cobalt and Lithium from Spent Lithium-Ion Batteries with Citric Acid. *Sep. Purif. Technol.* **2019**, *215*, 398–402. [CrossRef]
55. Musariri, B.; Akdogan, G.; Dorfling, C.; Bradshaw, S. Evaluating Organic Acids as Alternative Leaching Reagents for Metal Recovery from Lithium Ion Batteries. *Miner. Eng.* **2019**, *137*, 108–117. [CrossRef]
56. Chen, X.; Zhou, T. Hydrometallurgical Process for the Recovery of Metal Values from Spent Lithium-Ion Batteries in Citric Acid Media. *Waste Manag. Res. J. Sustain. Circ. Econ.* **2014**, *32*, 1083–1093. [CrossRef] [PubMed]
57. Chen, X.; Zhou, T.; Kong, J.; Fang, H.; Chen, Y. Separation and Recovery of Metal Values from Leach Liquor of Waste Lithium Nickel Cobalt Manganese Oxide Based Cathodes. *Sep. Purif. Technol.* **2015**, *141*, 76–83. [CrossRef]
58. Ma, L.; Nie, Z.; Xi, X.; Han, X. Hydrometallurgy Cobalt Recovery from Cobalt-Bearing Waste in Sulphuric and Citric Acid Systems. *Hydrometallurgy* **2013**, *136*, 1–7. [CrossRef]
59. Punt, T.; Akdogan, G.; Bradshaw, S.; van Wyk, P. Development of a Novel Solvent Extraction Process Using Citric Acid for Lithium-Ion Battery Recycling. *Miner. Eng.* **2021**, *173*, 107204. [CrossRef]
60. Gaines, L.L.; Dunn, J.B. Lithium-Ion Battery Environmental Impacts. In *Lithium-Ion Batteries: Advances and Applications*; Pistoia, G., Ed.; Elsevier: Amsterdam, The Netherlands, 2014; pp. 483–508; ISBN 9780444595133.